Hindawi Publishing Corporation
Journal of Nanomaterials
Volume 2016, Article ID 1847325, 12 pages
http://dx.doi.org/10.1155/2016/1847325

Research Article

Thermal Conductivity of Carbon Nanoreinforced Epoxy Composites

C. Kostagiannakopoulou, E. Fiamegkou, G. Sotiriadis, and V. Kostopoulos

Applied Mechanics Laboratory, Department of Mechanical Engineering and Aeronautics, University of Patras, University Campus, 26500 Patras, Greece

Correspondence should be addressed to V. Kostopoulos; kostopoulos@mech.upatras.gr

Received 8 February 2016; Revised 24 April 2016; Accepted 5 May 2016

Academic Editor: Shanxin Xiong

The present study attempts to investigate the influence of multiwalled carbon nanotubes (MWCNTs) and graphite nanoplatelets (GNPs) on thermal conductivity (TC) of nanoreinforced polymers and nanomodified carbon fiber epoxy composites (CFRPs). Loading levels from 1 to 3% wt. of MWCNTs and from 1 to 15% wt. of GNPs were used. The results indicate that TC of nanofilled epoxy composites increased with the increase of GNP content. Quantitatively, 176% and 48% increase of TC were achieved in nanoreinforced polymers and nanomodified CFRPs, respectively, with the addition of 15% wt. GNPs into the epoxy matrix. Finally, micromechanical models were applied in order to predict analytically the TC of polymers and CFRPs. Lewis-Nielsen model with optimized parameters provides results very close to the experimental ones in the case of polymers. As far as the composites are concerned, the Hashin and Clayton models proved to be sufficiently accurate for the prediction at lower filler contents.

1. Introduction

Fiber reinforced polymers (FRPs) are increasingly in demand as structural materials in the aerospace, automotive, and marine industries due to their high specific strength and stiffness. However these materials have shown limitation in application due to their poor, out-of-plane, performance which is dominated by the low toughness and insulating behavior of polymer matrix. Thus, in the last decade, researchers have focused on the incorporation of nanosized fillers into the matrix of FRPs in the sense of multiscale reinforcement in order to develop composites with improved mechanical, electrical, and thermal properties with the main purpose of creating multifunctional materials. Specifically, Arai et al. [1] reported that mode I interlaminar fracture toughness increased 50% by the presence of a carbon nanofiber interlayer into the CFRP composites. Furthermore, mode II interlaminar fracture toughness for doped laminates was 2-3 times greater than base CFRP laminates. Toward this direction, Karapappas et al. [2] observed that the addition of 1% wt. MWCNTs in CFRP composites improved mode I fracture toughness 63% while the introduction of 0.5% wt. MWCNTs in CFRPs caused the enhancement of 70% in mode II fracture toughness. In addition, Knoll et al. [3] investigated the influence of different carbon nanospecies like MWCNT and few layered graphene (FLG) on the damage mechanisms of CFRPs under fatigue loading. The results indicated a remarkable increase in fatigue life with the addition of low filler contents into the epoxy matrix of CFRPs. Similar research by Vavouliotis et al. [4] proved the positive effect on the fatigue life of CFRP composites with the incorporation of 0.5% wt. MWCNTs. In another work, Bekyarova et al. [5] verified an enhancement of 30% in interlaminar shear strength and a significant improvement in out-of-plane electrical conductivity after the addition of multi- and single-walled carbon nanotubes into the CFRP composites. Finally, Thostenson and Chou [6] exhibited significant enhancement in fracture toughness of CFRPs at low carbon nanotube concentrations and also reported the formation of a conductive percolating network at carbon nanotube concentrations below 0.1% wt. and an increase of 60% in thermal conductivity of CFRPs reinforced with 5% wt. carbon nanotubes.

In recent years thermal management has become a central task of academic and industrial interest for device design and

application. This is because many applications would benefit from the use of thermally conductive polymeric nanocomposites such as electronic packaging, heat exchangers, and satellite devices.

In order to enhance thermal conductivity of Polymeric Matrix Composites (PMCs) there is a tendency to incorporate thermally conductive nanofillers with high inherent thermal conductivity into the insulator polymer. The conductive fillers that are widely used to increase the thermal conductivity of polymers are based on ceramic, metallic, and carbon materials. Ceramic fillers appear to have high thermal conductivity but are expensive and inappropriate for many applications. Metal fillers are more affordable but increase the density of the final product. Consequently, the interest turned to conductive carbon additives such as carbon blacks (CBs), carbon nanofibers (CNFs), and carbon nanotubes (CNTs). For example, Han et al. [7] reported an increase of 63% in the through thickness thermal conductivity of CFRP composites doped with carbon black. Additionally, Joshi and Bhattacharyya [8] observed that the introduction of 1.5% wt. CNFs into CFRP composites improved by 35% their through thickness thermal conductivity.

The most widely used carbon nanospecies are carbon nanotubes (CNTs) due to their outstanding mechanical, electrical, and thermal properties. Also, their high aspect ratio and surface area make them unique. However, it has been observed that the incorporation of the above nanospecies into the polymer matrix of FRPs has significantly enhanced mechanical performance and electrical conductivity of final composite, but until now the desired enhancement in thermal conductivity has not been achieved. Thermal conductivity is a phonon based mechanism affected by many factors and not only by the thermal conductivity of each constituent. These factors are the geometry, orientation, volume fraction, and the dispersion of nanofillers into the polymer, as well as the interfacial thermal resistance between the phases [9, 10].

In the last few years, GNPs seem to be very promising nanoscaled conductive fillers since they combine the 2D effective layered structure with the superior thermal properties of carbon nanotubes. The above nanomaterials can be produced by graphite exfoliation, including mechanical cleavage of graphite, chemical exfoliation of graphite, and direct synthesis such as epitaxial growth [11]. Nevertheless, the need for large scale production of GNPs demonstrated chemical exfoliation as the most appropriate production method. Specifically, GNPs are disk-shaped graphite structures which are usually obtained by rapid heating of graphite intercalation compounds (GICs). The resulting material is composed of two or more layers of graphene planes and its platelet thickness ranges from 0.34 to 100 nm.

According to literature, the major advantage of GNPs is that their addition into the polymer enhances significantly the thermal conductivity of nanocomposites. Particularly, Yu et al. [12] presented a thermal conductivity enhancement of more than 3000% in epoxy nanocomposites by the incorporation of 25% vol. GNPs into the matrix. Kalaitzidou et al. [13] reported that polypropylene nanocomposites reinforced with 25% vol. xGNP showed 500% increase in thermal conductivity.

This extremely high improvement of thermal conductivity is very important because until now the cylindrical carbon structures (CNTs and CNFs) have not shown significant enhancement of this property after their integration in polymer nanocomposites. This is probably due to the fact that the 2D structure of GNPs provides reinforcement in 2 directions and a 2D path which is more effective for phonon transport than 1D path provided from CNTs [14, 15]. Finally, GNPs in contrast to CNTs do not cause a significant increase in polymer viscosity at high contents allowing better process conditions for the impregnation of the developed material. Thus, it is easier to prepare high content blends which are required in order to increase thermal conductivity of composites.

This study focuses on the incorporation of conductive fillers, GNPs and MWCNTs, in bulk epoxy resin and CFRP laminates with a purpose of improving their thermal conductivity. Also, one of the main objectives of this work was to investigate which of the above two nanoadditives is more efficient in this field. Finally, the effectiveness of selected micromechanical models in predicting the thermal conductivity of the produced materials was investigated.

2. Experimental Section

2.1. Materials. The matrix material, used in this study, was a four-component epoxy B-staging system supplied by Huntsman Advanced Materials, Switzerland. This system contains the low-viscosity epoxy resin Araldite LY1556, the hardener paste Aradur 1571, the accelerator paste 1573, and the polyamine hardener Aradur XB 3403. The components were mixed by weight at a ratio of 100/23/5/12 according to the instructions of the manufacturer. The GNPs were provided by Cheap Tubes Inc., USA. GNPs consisted of 20–25 graphene layers with an average thickness of 10–12 nm and a typical diameter of 5 microns, while their surface area was about 100 m^2/g. MWCNTs were produced by catalyzed chemical vapor deposition, CVD, and were supplied by ARKEMA, France. Their diameters were 10–15 nm, their typical length was more than 500 nm long, and their surface area was approximately 230 m^2/g. Finally, a unidirectional noncrimp carbon fabric, supplied by R&G, Germany, with an areal density of 140 g/m^2 and TORAY T300 fiber, was used as the reinforcement of the composites.

2.2. Preparation of Isotropic Samples. The dispersion of nanofillers into the epoxy resin was realized utilising a dissolver device (Dispermat AE, VMA Getzmann GmbH). This technique leads to the introduction of high shear forces and vortex flow in the mixture during stirring. This fact contributes to the efficient reduction of agglomeration of the nanofillers and the development of homogeneous mixtures. For the production of nanodoped compounds with different weight fractions, the masterbatch approach was followed. The preparation of the masterbatches (20% wt. GNPs and 4% wt. MWCNTs) was carried out in a vacuum container in order to eliminate the entrapped air during mixing. The speed was maintained at 2500 rpm for 7 h while the temperature

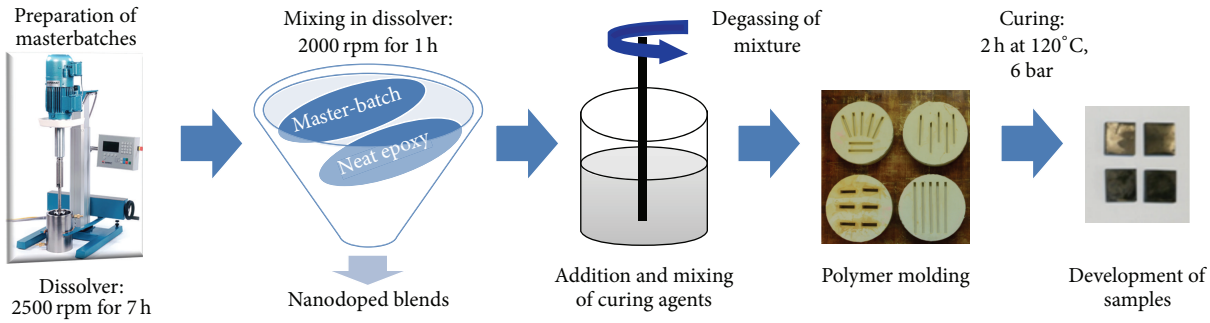

Figure 1: Schematic presentation of the preparation of isotropic samples.

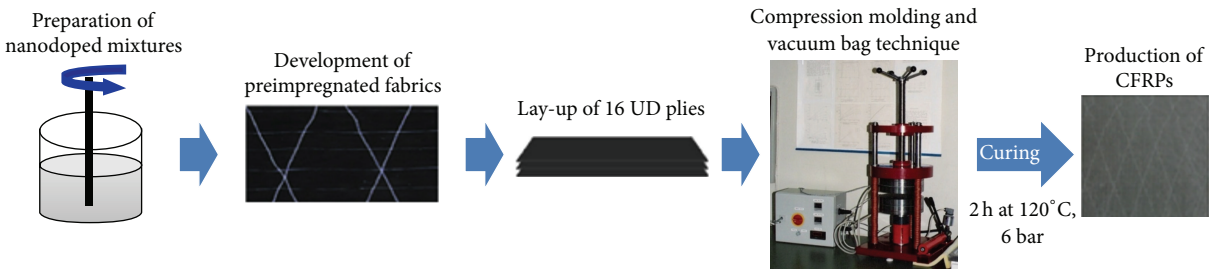

Figure 2: Schematic presentation of the preparation of nanomodified CFRPs.

of the mixture was kept constant at 60°C. Afterwards, the appropriate amounts of the prepared masterbatches and neat epoxy resin were mixed in dissolver at 2000 rpm for 1 h with the purpose of producing nanodoped compounds with different filler loading levels. The other three parts of the prepreg system were subsequently added to the mixture and placed again in a vacuum chamber for final degassing. Then, the produced mixture was poured in silicon rubber molds and cured, according to manufacturer's recommended curing cycle (2 h at 120°C). Following the aforementioned process, two different types of isotropic nanocomposites of different weight fractions were developed: 1, 3, 5, 10, and 15% wt. GNPs and 1 and 3% wt. MWCNTs. Neat epoxy samples were also produced for reference. The step by step preparation of isotropic samples is presented in Figure 1.

It is worth noting that the preparation of MWCNT compounds at similar high content levels to those of GNP compounds was not achieved. This is due to the fact that the processing of CNT-masterbatch at loadings higher than 4% wt. proved almost impossible for the particular mixing process. The introduction of higher loadings of MWCNTs into the epoxy resin increased dramatically the viscosity of the mixture, resulting in a nonstirrable mixture. This is a consequence of the tendency of MWCNTs, caused by their tubular geometry, to form agglomerates more easily than GNPs at higher contents.

2.3. Preparation of Carbon-Reinforced Nanomodified Epoxy Laminates. Firstly, the uncured nanomodified system was used for the impregnation of unidirectional fabrics with a view to produce prepregs. The fabric impregnation was carried out manually, at room temperature, while the B-staging succeeded by keeping the prepreg for 48 h at 20°C and 55% to 65% RH. Next, they were placed in the freezer at −18°C. Then, the prepregs were cut and laminated for the production of nanomodified CFRPs. Each plate consisted of 16 layers and their curing was carried out combining the compression molding method with the vacuum bag technique in appropriate temperature and pressure profile (120°C for 2 h and 6-bar pressure). Reference composites plates were also manufactured using the same procedure. The step by step production of carbon-reinforced nanomodified epoxy laminates is presented in Figure 2.

2.4. Instrumentation and Characterization. Thermal conductivity of the developed materials was measured by using a thermal conductivity analyzer (TCi Mathis). TCi Mathis Analyzer measures directly and rapidly the through thickness thermal conductivity of a sample at room temperature, providing a detailed overview of its thermal characteristics. Its operation is based on a known current which is applied to the sensor's heating element, providing a small amount of heat flux that causes a temperature increase at the interface between the sensor and the sample. This increase induces a change in the voltage drop of the sensor element and the increasing rate in the sensor voltage is used for the determination of thermal conductivity of samples. Four specimens were measured for each material type. The dimensions of the measured samples were 25 mm × 25 mm × 5 mm in the case of nanoreinforced polymers and 25 mm × 25 mm × 2 mm in the case of nanomodified laminates. Finally, the microstructure of cryogenic fracture surfaces of the tested coupons was analyzed by using a LEO SUPRA 35VP Scanning Electron Microscope (SEM).

Table 1: Thermal conductivity values of nanoreinforced polymers.

Samples	Thermal conductivity		
	Average [$Wm^{-1}\cdot K^{-1}$]	Increase [%]	Standard deviation
Neat	0.29	—	0.01
1% wt. MWCNTs	0.31	7	0.02
3% wt. MWCNTs	0.36	24	0.03
1% wt. GNPs	0.32	10	0.01
3% wt. GNPs	0.41	41	0.02
5% wt. GNPs	0.49	69	0.01
10% wt. GNPs	0.63	117	0.03
15% wt. GNPs	0.80	176	0.08

3. Results and Discussion

3.1. Thermal Conductivity of Nanoreinforced Polymers. Table 1 presents the results of thermal conductivity of the produced reference and nanoreinforced polymer materials. It is observed that the incorporation of both carbon fillers increase the thermal conductivity of the reference polymer. Furthermore, thermal conductivity of the epoxy system was increased significantly by increasing the filler content. As can be seen in Figure 3 the highest increase (~176%) in thermal conductivity was achieved in the case of 15% wt. GNP-reinforced epoxy. However, it is worth mentioning that the addition of GNPs enhanced more efficiently the thermal conductivity of polymer in comparison to the MWCNTs. As it is shown in Table 1, the integration of 3% wt. GNPs increased by 41% the thermal conductivity of the polymer while the addition of MWCNTs at the same content resulted in an increase of the thermal conductivity of the polymer at the level of 24%. GNPs seem to be more promising fillers than MWCNTs for the production of thermally conductive polymers and there are two direct explanations for this fact. (1) The 2D platelet shape of GNPs offers advantages in thermal conductivity concerning the others' spherical or cylindrical morphologies. In particular, GNPs due to their flat shape have higher effective contact surface area than CNTs where point contact is achieved; thus they can efficiently embed into the matrix permitting much closer areal contact between adjacent platelets. Hence, the thin polymer layer between fillers, which is responsible for the phonon scattering due to the conductivity mismatch between the thermally conductive fillers and the insulating polymer matrix, is reduced. Also, the disk-shaped GNPs provide 2D path contributing to more effective phonon transport than the 1D path and the point contact provided by the CNTs [14, 15]. (2) The addition of flat-shaped GNPs into polymers has a much smaller effect on the viscosity in comparison to the incorporation of tubular-shaped CNTs. This allows better processing windows for the incorporation of higher contents (>5%) which is necessary in order to achieve higher increase in thermal conductivity [9]. At the same time the resulting agglomerates are limited in the case of GNPs; CNTs cannot reach these contents because they show high entanglement, due to their 1D tubular structure even at relatively lower contents (>1%) inside the polymer.

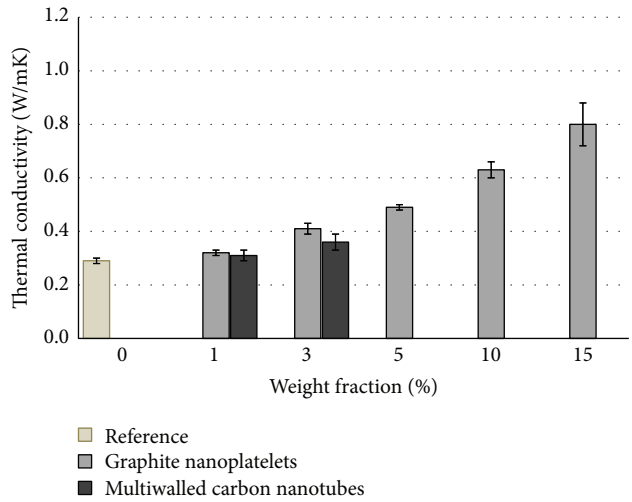

Figure 3: Thermal conductivity of nanoreinforced polymers.

Thus, the manufacturing of high content CNT polymer is prohibited.

The representative SEM micrographs of the nanoreinforced polymers filled with different weight contents of GNPs and CNTs are shown in Figures 4 and 5, respectively. Firstly, it can be seen that the polymers containing carbon nanospecies exhibit rougher matrix fracture surfaces compared to the neat epoxy, a fact attributed to the more macroscopically ductile failure of the nanodoped materials. Also, SEM images were used for a statistical estimation of dispersion of the carbon nanospecies in epoxy matrix. It can be shown from the figures that the nanofillers are fairly well dispersed in the nanoreinforced polymers; however it is observed that the increasing filler content in the epoxy leads to the creation of more intense aggregation between the particles.

3.2. Thermal Conductivity of Nanomodified Composites. Table 2 presents the results of through thickness thermal conductivity of the produced nanomodified composites which are reinforced with GNPs and MWCNTs. At low loading levels (1 and 3% wt.) of carbon fillers, the thermal conductivity remains almost unaffected and any differences are within the statistical error. However GNPs at higher contents (5, 10, and 15% wt.) improved greatly the thermal behavior of CFRPs with the highest increase (48%) obtained from the nanomodified composite with GNP content of 15% wt. This was expected taking into account the thermal conductivity increase that was achieved in polymers by the addition of same-level GNPs.

4. Micromechanical Modeling of Thermal Conductivity

4.1. Micromechanical Models. In the present part of the work some very popular micromechanical models were tested in order to compare their effectiveness against the experimentally obtained thermal conductivity (TC) in the case of nanoreinforced polymers as well as in the case of the through

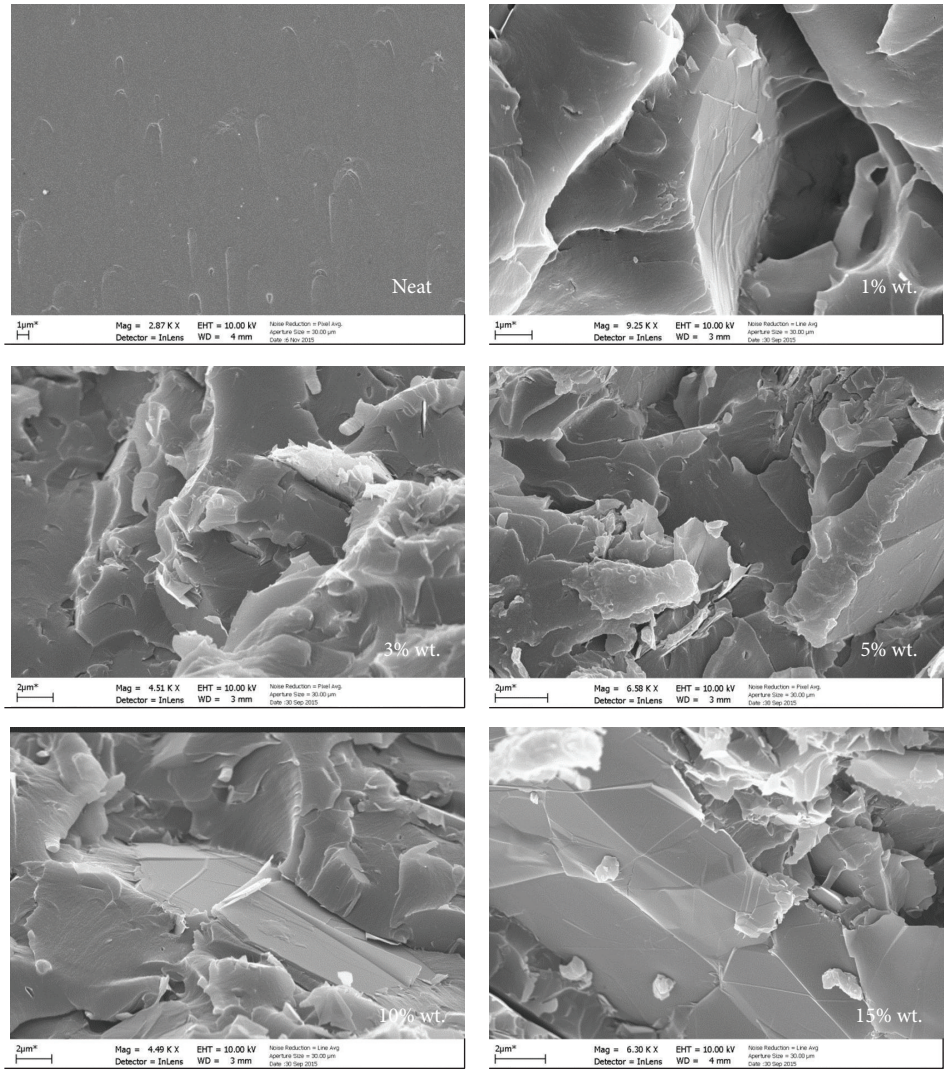

Figure 4: SEM images of the reference and nanoreinforced polymers filled with different contents of GNPs.

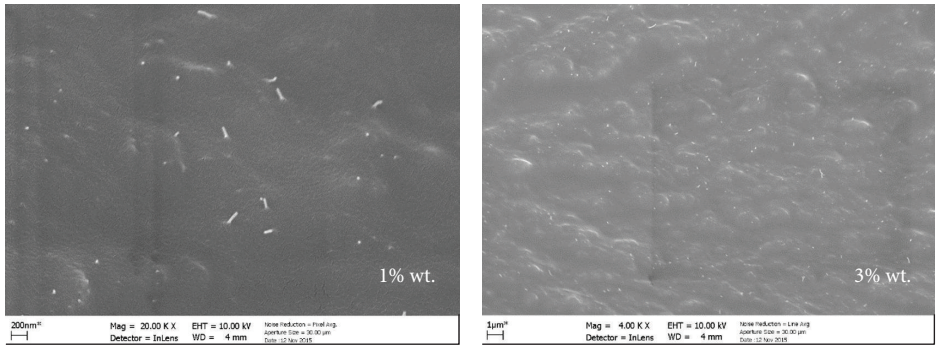

Figure 5: SEM images of the nanoreinforced polymers filled with different contents of MWCNTs.

thickness thermal conductivity nanomodified composites. Explanations for the convergence of some of the investigated models to the experimental results were discussed analytically. Basic modifications were also proposed for taking into account the nanoscale size of the reinforcements.

Tables 3 and 4 present the TC models tested for the nanoreinforced polymers and nanomodified composites, respectively. These models could be classified in three different groups. The first group includes models that are only based on the thermal conductivity of the constituents and their volume

Table 2: Thermal conductivity values of nanomodified composites.

Samples	Thermal conductivity		
	Average [$Wm^{-1}\cdot K^{-1}$]	Increase [%]	Standard deviation
Neat	0.65	—	0.05
1% wt. MWCNTs	0.63	−3	0.03
3% wt. MWCNTs	0.62	−5	0.03
1% wt. GNPs	0.65	0	0.05
3% wt. GNPs	0.68	5	0.08
5% wt. GNPs	0.73	12	0.05
10% wt. GNPs	0.86	32	0.07
15% wt. GNPs	0.96	48	0.04

fractions (TCI). The second group (TCII) includes models where also the size, geometry, dimensions, and the aspect ratio of filler are taken into account. Finally, the third group of models (TCIII) takes into account the interfacial thermal resistance between filler and matrix. All the considered models are based on the following assumptions: (a) the heat energy transfer between phases takes place through conduction; (b) the discontinuous phase (reinforcement) is homogeneously dispersed in continuous phase (matrix); (c) the nanoreinforced polymers have been considered macroscopically homogeneous and thermally isotropic; (d) the UD nanomodified composites have been considered macroscopically transversely thermally isotropic; (e) for the Halpin-Tsai model, MWCNTs have been considered as short fibers due to their shape [17], where, in all cases, the following notations have been used: K is equivalent thermal conductivity (for the CFRPs only in the through thickness direction); k_m is thermal conductivity of matrix; k_f is thermal conductivity of filler; v_m is matrix volume fraction; v_f is filler volume fraction (for the CFRPs: fiber volume fraction).

The filler volume fraction (v_f) of nanoreinforced polymers was calculated by using the following equation:

$$v_f = \frac{w_f/\rho_f}{w_f/\rho_f + w_m/\rho_m}, \quad (1)$$

where w_m is matrix weight fraction; w_f is filler weight fraction; ρ_m is matrix density (~1.15 g/cm^3); ρ_f is filler density (GNPs = 2 g/cm^3, MWCNTs = 2.092 g/cm^3).

Parallel model maximizes the contribution of the conductive phase because it assumes perfect contact between particles. Generally it does not predict well the thermal conductivity of the nanoreinforced material, since in many cases it concludes to significant overestimations of K. The basic series model assumes no contact between particles and thus the contribution of particles is confined to the region of matrix embedding the particle. This model usually achieves better convergence to experimental results compared to the parallel model. Geometric model usually fits the experimental results much better than the parallel and the basic series model at low content [10]. However, it shows large deviation from experimental values at higher filler loadings. Halpin-Tsai model is a widely thermal transport formula for transverse thermal conductivity. It takes into account the geometry of filler by using parameter ξ. Its value depends on the filler shape. For multilayer platelets parameter ξ is calculated by using the equation $\xi = \sqrt{3}\log(a/b)$, where a and b are the width and thickness of platelet, respectively, while for cylindrical nanotubes ξ is equal to 1 [17] according to assumption (e) mentioned earlier. Lewis and Nielsen model is based on Halpin-Tsai equation. Nielsen model includes the additional parameter "Ψ" in order to take into consideration the orientation and the packing of the filler in the matrix. "Φ_m" term is the maximum volumetric packing fraction of the filler while "A" parameter takes into account the geometry, specifically the aspect ratio, and the orientation of the filler. "A" and "Φ_m" terms have already been calculated for some filler types and orientation and are available in literature [10]. Regarding the GNPs, the selection of values was made considering these fillers as plates for the determination of A [18] and the packing order of random close (irregular shape) in the case of Φ_m [10]. MWCNTs were considered as random fibers with the lower aspect ratio of 15 for the determination of A and the packing order of three-dimensional random (fiber shape) in the case of Φ_m [10]. Prasher model except from particle size takes into account the interfacial thermal resistance between filler and matrix. Bi is the Biot number that is calculated from the interfacial resistance "R_k" and diameter of nanospecies "d." The values of "R_k" that are used for testing the Prasher model are obtained from literature [9, 19].

Furthermore, Hashin and Clayton models predict the through thickness thermal conductivity of unidirectional composites laminates. Hashin model assumes that fibers can be also transversely isotropic, which is the case of carbon fibers. The fiber volume fractions (v_f) that were used in order to calculate the through thickness thermal conductivity of nanomodified composites using the above models are shown in Table 5. In addition, the v_f used for the calculation of the thermal conductivity of CFRP with the nonmodified matrix was 58%. These fiber volume fractions were derived by using (1) in combination with the use of dimensional and weight characteristics of the produced CFRPs and technical information of the as-received materials (carbon fabric and polymer system). Furthermore, optical microscopy and image analysis software were also used to confirm the concluded v_f.

Finally, Table 6 summarizes the reference thermal conductivity values of the constituent materials that have been inputted in micromechanical models as k_m and k_f for the prediction of thermal conductivity of nanomodified polymers. These values derived from the material datasheets, which are provided by the manufacturers of the materials. For the same purpose in the case of UD nanomodified composites, the measured nanoreinforced polymer thermal conductivity value was used as the value for k_m and the thermal conductivity of the fiber was used as k_f in the transverse direction. In the present case the thermal conductivity of fiber in transverse direction was taken as 15 times lower than the conductivity in axial direction [20].

4.2. Results and Discussion

4.2.1. TC Models Applied to Nanoreinforced Polymers. Figures 7–9 present the results obtained by using the different groups

Table 3: Micromechanical models tested for nanoreinforced polymers.

Group	Model	Equation	Notes
TCI	Rule of Mixtures	*Parallel model:* $K = k_f v_f + k_m v_m$ *Basic series model:* $\frac{1}{K_T} = \frac{v_f}{k_f} + \frac{v_m}{k_m}$ *Geometric mean model:* $K = k_f^{v_f} \cdot k_m^{v_m}$	*Parallel model:* perfect contact between particles *Basic series model:* no contact between particles *Geometric mean model:* no contact between particles
TCII	Halpin-Tsai	$K = k_m \left[\frac{1 + \xi\eta v_f}{1 - \eta v_f}\right], \quad \eta = \frac{(k_f/k_m) - 1}{(k_f/k_m) + \xi}$	*GNPs*: $\xi = \sqrt{3}\log\left(\frac{a}{b}\right)$ *MWCNTs:* $\xi = 1$
	Lewis-Nielsen	$K = k_m\left(\frac{1 + A \cdot B \cdot v_f}{1 - B \cdot v_f \cdot \psi}\right)$ $B = \frac{k_f/k_m - 1}{k_f/k_m + A}, \quad \psi = 1 + \left(\frac{1 - \varphi_m}{\varphi_m^2}\right) v_f$	*GNPs:* $A = 7.72$, $\varphi_m = 0.637$ *MWCNTs:* $A = 8.38$, $\varphi_m = 0.52$
TCIII	Prasher	$K = \frac{k_m}{(1 - v_f)^{3(1-\mathrm{Bi})/(1+2\mathrm{Bi})}}, \quad \mathrm{Bi} = \frac{R_k k_m}{d}$	*GNPs:* $R_k = 15 - 30 * 10^{-8}$ m^2 K/W [16] *MWCNTs:* $R_k = 7 * 10^{-7}$ m^2 K/W

Table 4: Micromechanical models tested for nanomodified composites.

Group	Model	Equation	Notes
TCI	Hashin	$K = k_m\left[\frac{k_m v_m + k_f(1 + v_f)}{k_m(1 + v_f) + k_f v_m}\right]$	Fibers: transversely isotropic
	Clayton	$K = \frac{k_m}{4}\left[\sqrt{(1 - v_f)^2\left(\frac{k_f}{k_m} - 1\right)^2 + \frac{4k_f}{k_m}} - (1 - v_f)\left(\frac{k_f}{k_m} - 1\right)\right]^2$	

Table 5: Fiber volume fractions of nanomodified composites.

	Fiber volume fractions (v_f), %	
w_f (%)	GNPs	MWCNTs
1	58	58
3	63	50
5	60	—
10	52	—
15	47	—

Table 6: Thermal conductivity values of matrix and reinforcements.

	Thermal conductivity values
Material	k (W/mK)
Epoxy system	0.29
Graphene nanoplatelets	3000
Multiwalled carbon nanotubes	3000
Carbon fibers	0.915

of micromechanical models in order to predict thermal conductivity of GNP-reinforced polymers. A comparison between experimental and theoretical values is given for evaluating validity of the applied models. Initially it should be mentioned that the results for the parallel model are not included in Figure 7. The parallel model overestimates TC values in a way that puts them out of the useful scale of the graph of Figure 7. Regarding the results of the predictive models, the thermal conductivity of GNP-reinforced polymers is observed to increase while increasing the content of fillers, as expected.

Figure 7 shows the results obtained based on the first group of models (TCI). It is evident that the series model significantly underestimates the experimental data and does not follow the rate of increasing conductivity increasing GNP content. On the other hand, the geometric model approaches better the experimental results, although there is again a constant underestimation of the experimental data.

The results concluded by the application of second group of models (TCII) are given in Figure 8. As illustrated, Lewis-Nielsen model provides higher TC values compared against Halpin-Tsai model and better approaches the experimental results although still there is a significant underestimation. This is reasonable behavior considering that the Lewis-Nielsen model resulted from Halpin-Tsai equation by incorporating the orientation (A) and the packing (Φ_m) of the filler as extra parameters for the better prediction of thermal conductivity of a multiphase composite.

Finally, Figure 9 shows the behavior of Prasher model, which belongs to the last group (TCIII) of predictive models. It can be seen that this model fits only the experimental data at the content of 1% wt. GNPs however present large deviations at higher filler loadings (>1% wt.). Possibly, this is due to the fact that the model is very insensitive for $R_k > 10^{-8}$ m^2 K/W, which corresponds to higher loadings of carbon fillers. At higher contents the effective aspect ratio of fillers reduces, decreasing the contact area between filler and matrix, due to the presence of agglomerates. According to the literature, there is a strong influence of aspect ratio of carbon fillers on the thermal conductivity of nanoreinforced polymers. Large aspect ratio results in an increased probability of contact of the carbon nanospecies minimizing the polymer matrix in between, which improves the carbon filler-polymer interaction and reduces significantly R_k across the filler-matrix interface, which is responsible for the degradation of thermal conductivity property [16, 21]. Taking into consideration (a) the increase of R_k by increasing the content of carbon fillers into the polymer [19], (b) the insensitivity that presents this model for $R_k > 10^{-8}$ m^2 K/W that corresponds to higher contents, and (c) significantly better convergence of the model prediction to the experimental data at filler content of 1% wt. compared to that of the higher filler contents, we can claim that the enhancement of thermal conductivity at higher filler contents depends more on the filler shape and the contact distance between adjacent particles (formation of more phonon paths at higher contents) than on the interfacial thermal resistance between filler and matrix. This fact explains the increase of thermal conductivity with increasing filler content as concluded from the experiments. Thus Prasher model is not adequate for the prediction of the thermal conductivity of carbon nanoreinforced polymer at higher contents. In Figure 10 a comparative plot is given for all the models (initial, nonparameterized) and the experimental data. The same increasing trend is evident in all models. The better fit is observed for the geometrical one. However, the parameterized Lewis-Nielsen finally yielded the best results (Figure 11). In order for the Lewis-Nielsen model to converge to the experimental results in the case of the GNP nanospecies used in the present work, an optimization scheme was applied for both the parameters of the model: the packing factor Φ_m and the aspect ratio A. The parameters A and Φ_m were optimized by using the Nelder-Mead Simplex method as well as via Genetic Algorithms [22]. The results obtained from both methods were almost identical. The A factor was optimized with the constraint that this value had to be greater than or equal to zero. Furthermore, the Φ_m factor was optimized with the constraint that the value had to be greater than or equal to zero and simultaneously lower than or equal to one. The optimization process results as 16.93 for parameter A and 0.741 for parameter Φ_m in order to achieve the minimum RMSE (root min square error) given the experimental data. Figure 11 presents the resulting convergence between Lewis-Nielsen model and the experimental results in the cases of GNP nanocomposites after parameter optimization for the values of thermal conductivity.

Figures 12, 13, and 14 present the application of the three different groups of models for the prediction of TC against experimental results in MWCNTs nanopolymers. A comparative plot is given in Figure 15 for all the models' predictions and the experimental data. In the case of MWCNT-reinforced polymers the geometrical along with Lewis-Nielsen models give better predictions of the thermal conductivity of the nanocomposites. However in the case of Lewis-Nielsen model, the used values from the literature for the packing factor and the aspect ratio [10] do not represent the characteristics of the used MWCNTs and their final arrangement within the nanocomposites. Thus, considering a random orientation of the MWCNT nanospecies, which leads to Φ_m equal to 0.52, and taking into consideration the different aspect ratio of MWCNTs used in the present study which was within the range of 20–50, the optimized A value was found to be $A = 13.03$. Figure 16 shows the resulting convergence between Lewis-Nielsen model and the experimental results after parameter optimization, in the case of thermal conductivity of MWCNT nanocomposites.

4.2.2. TC Models Tested for Nanomodified Composites. Figures 17 and 18 present the results obtained for the through thickness thermal conductivity of CFRPs with nanomodified epoxy matrix with GNPs and MWCNTs, respectively. The presented results come from the application of phenomenological analytical models proposed by Hashin and Clayton (Table 4) and they were compared against experimental data given in Figure 6. It is evident that both models fit sufficiently well the experimental results at low filler content into the epoxy matrix. However, both show large deviation at higher filler loadings (>5% wt.) in the case of GNP doping of polymers. Furthermore, as it is evident in Figures 17 and 18, the above models provide almost similar predictions in the case of both nanomodified CFRPs.

5. Conclusions

The work studies the variation of thermal conductivity of polymers and polymer matrix composites due to the nanomodification of the polymer material by the incorporation of carbon based nanospecies at various % wt. levels.

The results indicate that the thermal conductivity of nanoreinforced epoxy polymers increases with increasing content of carbon nanospecies into the polymer. GNPs showed higher enhancements than MWCNTs due to their 2D effective platelet shape for phonon transport and their better distribution at higher contents inside the polymer. The addition of 15% wt. GNPs into the epoxy matrix in the case of nanoreinforced polymers was found to increase by 176% the thermal conductivity.

Concerning the nanodoped carbon fiber epoxy composites, the incorporation of nanospecies improved their through thickness thermal conductivity. At contents higher than 1% wt., MWCNTs were not effective in improving the thermal conductivity of CFRPs. The highest increase of the through thickness thermal conductivity of CFRPs was achieved by the integration of 15% wt. GNPs into the epoxy matrix resulting in an enhancement of 48%.

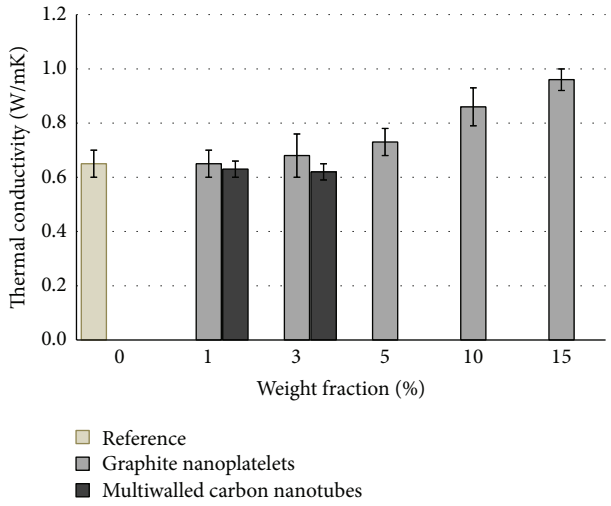

Figure 6: Thermal conductivity of nanomodified composites.

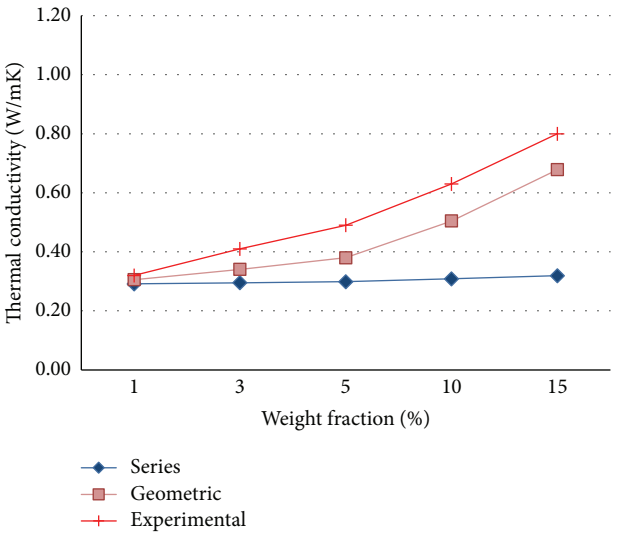

Figure 7: Thermal conductivity of GNP-reinforced polymers, Group TCI.

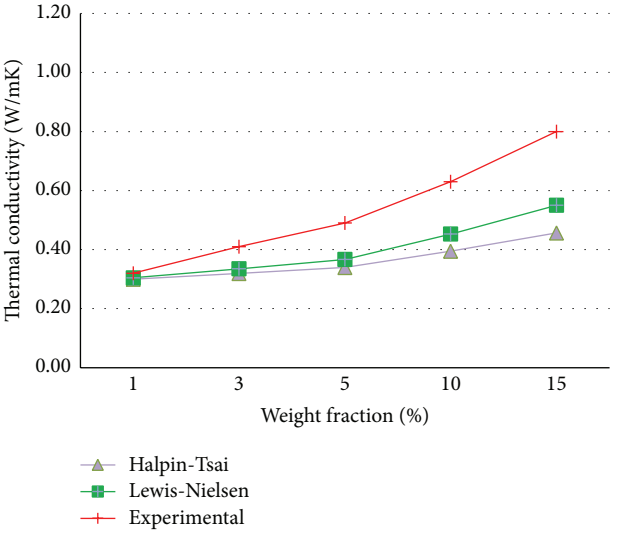

Figure 8: Thermal conductivity of GNP-reinforced polymers, Group TCII.

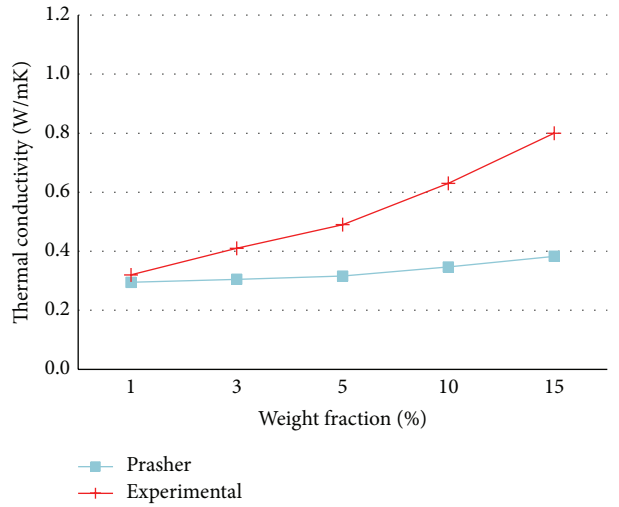

Figure 9: Thermal conductivity of GNP-reinforced polymers, Group TCIII.

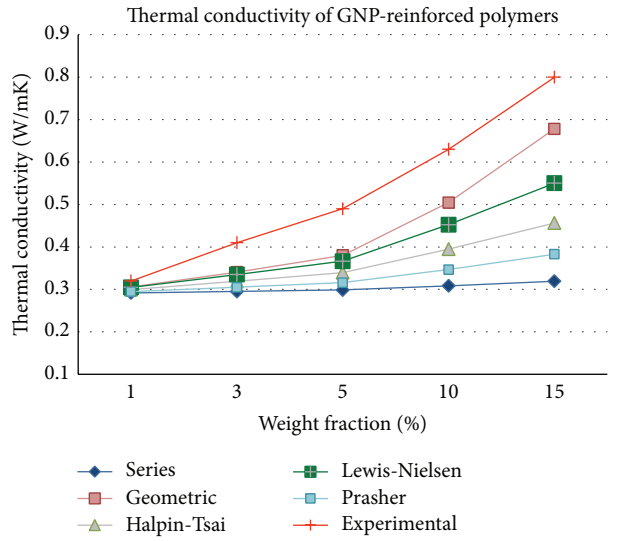

Figure 10: Comparative plot of all models and experimental values of GNP-reinforced polymers.

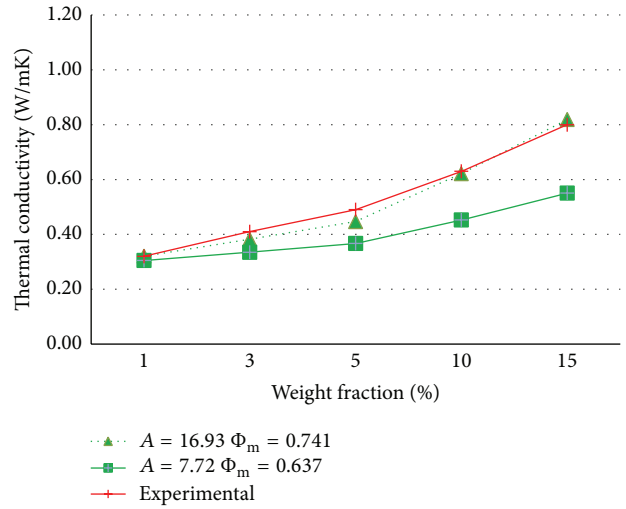

Figure 11: Thermal conductivity of GNP-reinforced polymers by using Lewis-Nielsen model with optimized A and Φ_m.

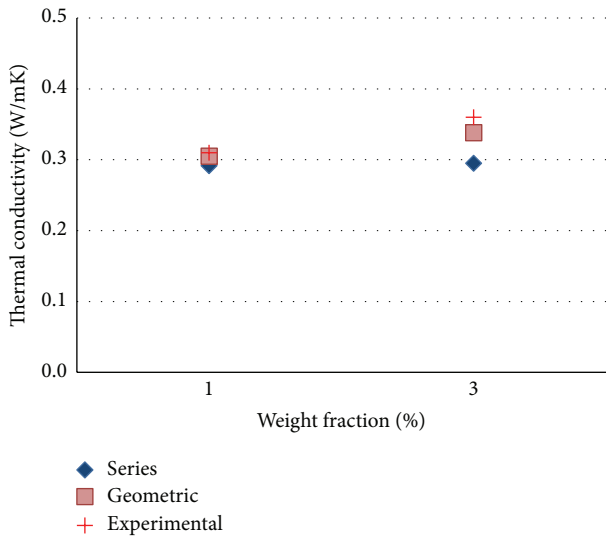

Figure 12: Thermal conductivity of MWCNT-reinforced polymers, Group TCI.

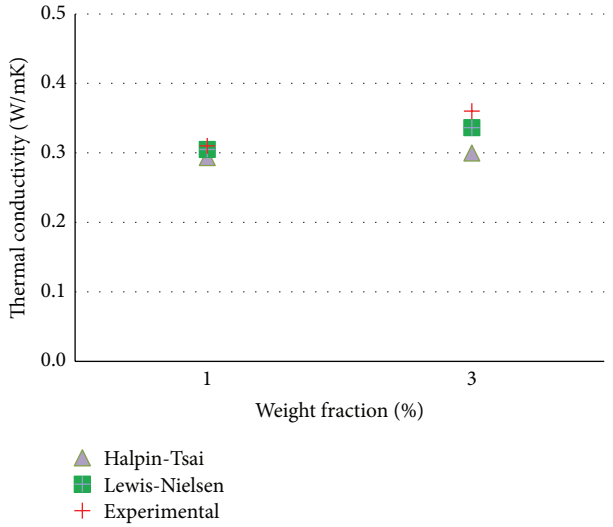

Figure 13: Thermal conductivity of MWCNT-reinforced polymers, Group TCII.

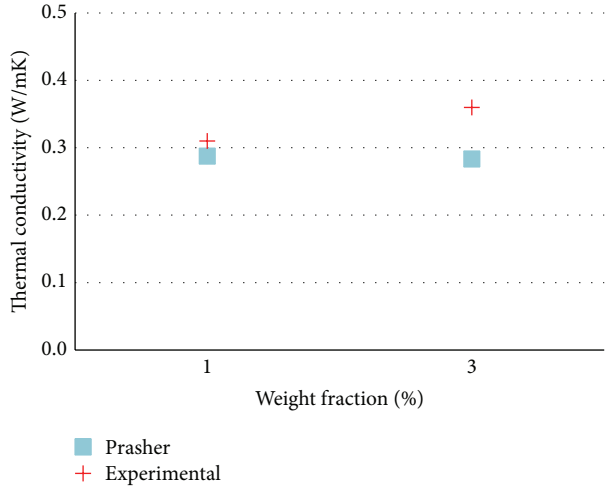

Figure 14: Thermal conductivity of MWCNT-reinforced polymers, Group TCIII.

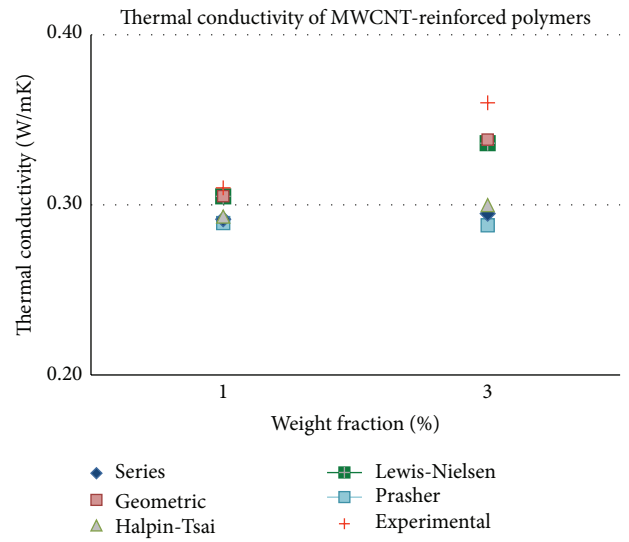

Figure 15: Comparative plot of all models and experimental values of GNP-reinforced polymers.

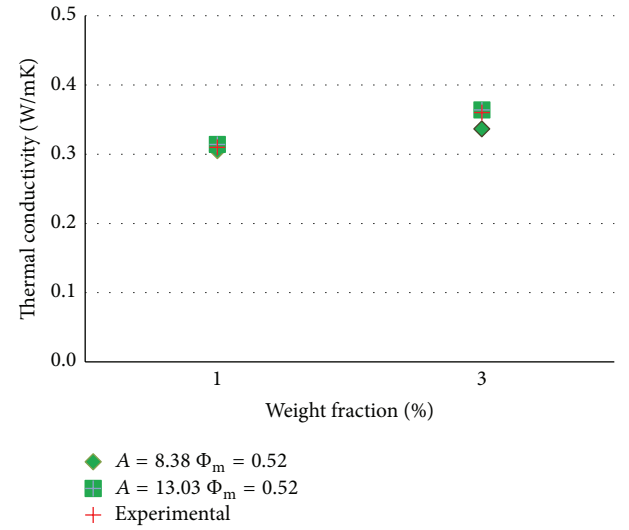

Figure 16: Thermal conductivity of MWCNTs-reinforced polymers by using Lewis-Nielsen model with optimized A.

Regarding the micromechanical models, the modified Lewis-Nielsen model proved the most efficient for the prediction of the thermal conductivity of nanoreinforced polymers while in the case of nanomodified composites the results of the tested Hashin and Clayton models fit nicely the experimental data, especially at lower filler contents (<5% wt.).

Competing Interests

The authors declare that there are no competing interests regarding the publication of this paper.

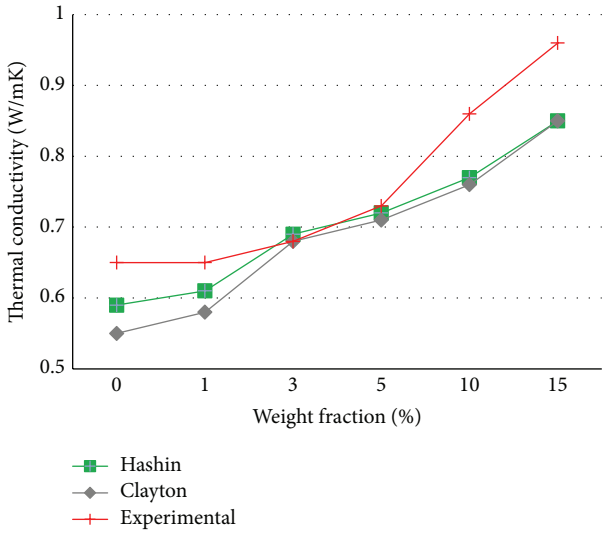

FIGURE 17: Thermal conductivity results of GNP-reinforced composites, Group TCI.

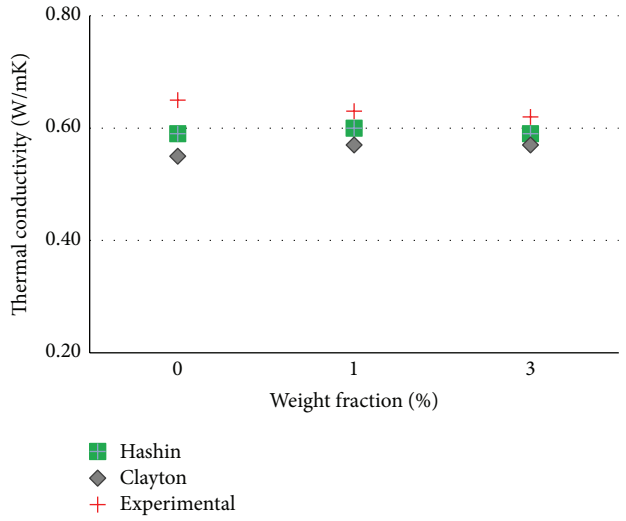

FIGURE 18: Thermal conductivity results of MWCNTs-reinforced composites, Group TCI.

Acknowledgments

The present work was partially supported by FP7 Project under the acronym SARISTU (Smart Intelligent Aircraft Structures). The authors would like to gratefully acknowledge the support of Mr. Nikolaos Eleftheroglou for his valuable contribution in the present study.

References

[1] M. Arai, Y. Noro, K.-I. Sugimoto, and M. Endo, "Mode I and mode II interlaminar fracture toughness of CFRP laminates toughened by carbon nanofiber interlayer," *Composites Science and Technology*, vol. 68, no. 2, pp. 516–525, 2008.

[2] P. Karapappas, A. Vavouliotis, P. Tsotra, V. Kostopoulos, and A. Paipetis, "Enhanced fracture properties of carbon reinforced composites by the addition of multi-wall carbon nanotubes," *Journal of Composite Materials*, vol. 43, no. 9, pp. 977–985, 2009.

[3] J. B. Knoll, B. T. Riecken, N. Kosmann, S. Chandrasekaran, K. Schulte, and B. Fiedler, "The effect of carbon nanoparticles on the fatigue performance of carbon fibre reinforced epoxy," *Composites Part A: Applied Science and Manufacturing*, vol. 67, pp. 233–240, 2014.

[4] A. Vavouliotis, P. Karapappas, T. Loutas, T. Voyatzi, A. Paipetis, and V. Kostopoulos, "Multistage fatigue life monitoring on carbon fibre reinforced polymers enhanced with multiwall carbon nanotubes," *Plastics, Rubber and Composites*, vol. 38, no. 2–4, pp. 124–130, 2009.

[5] E. Bekyarova, E. T. Thostenson, A. Yu et al., "Multiscale carbon nanotube-carbon fiber reinforcement for advanced epoxy composites," *Langmuir*, vol. 23, no. 7, pp. 3970–3974, 2007.

[6] E. T. Thostenson and T.-W. Chou, "Processing-structure-multi-functional property relationship in carbon nanotube/epoxy composites," *Carbon*, vol. 44, no. 14, pp. 3022–3029, 2006.

[7] S. Han, J. T. Lin, Y. Yamada, and D. D. L. Chung, "Enhancing the thermal conductivity and compressive modulus of carbon fiber polymer-matrix composites in the through-thickness direction by nanostructuring the interlaminar interface with carbon black," *Carbon*, vol. 46, no. 7, pp. 1060–1071, 2008.

[8] M. Joshi and A. Bhattacharyya, "Carbon nanofiber reinforced carbon/polymer composite," *Nanotech*, vol. 3, no. 6, pp. 308–311, 2004.

[9] Sh. J. J. Nejad, "A review on modeling of the thermal conductivity of polymeric nanocomposites," *e-Polymers*, vol. 12, no. 1, pp. 253c–288c, 2012.

[10] E. H. Weber, *Development and modeling of thermally conductive polymer/carbon composites [Bachelor of Science]*, Michigan Technological University, 1999.

[11] H. Kim, A. A. Abdala, and C. W. MacOsko, "Graphene/polymer nanocomposites," *Macromolecules*, vol. 43, no. 16, pp. 6515–6530, 2010.

[12] A. Yu, P. Ramesh, X. Sun, E. Bekyarova, M. E. Itkis, and R. C. Haddon, "Enhanced thermal conductivity in a hybrid graphite nanoplatelet—carbon nanotube filler for epoxy composites," *Advanced Materials*, vol. 20, no. 24, pp. 4740–4744, 2008.

[13] K. Kalaitzidou, H. Fukushima, and L. T. Drzal, "Mechanical properties and morphological characterization of exfoliated graphite-polypropylene nanocomposites," *Composites Part A: Applied Science and Manufacturing*, vol. 38, no. 7, pp. 1675–1682, 2007.

[14] S.-Y. Yang, W.-N. Lin, Y.-L. Huang et al., "Synergetic effects of graphene platelets and carbon nanotubes on the mechanical and thermal properties of epoxy composites," *Carbon*, vol. 49, no. 3, pp. 793–803, 2011.

[15] A. Yu, P. Ramesh, X. Sun, E. Bekyarova, M. E. Itkis, and R. C. Haddon, "Enhanced thermal conductivity in a hybrid graphite nanoplatelet-carbon nanotube filler for epoxy composites," *Advanced Materials*, vol. 20, no. 24, pp. 4740–4744, 2008.

[16] W. Lin, R. Zhang, and C. P. Wong, "Modeling of thermal conductivity of graphite nanosheet composites," *Journal of Electronic Materials*, vol. 39, no. 3, pp. 268–272, 2010.

[17] M. Zimmer, X. Fan, J. Bao et al., "Through-thickness thermal conductivity prediction study on nanocomposites and multi-scale composites," *Materials Science and Applications*, vol. 3, no. 3, pp. 131–138, 2012.

[18] S. H. Katz and V. J. Milewski, *Handbook of Fillers for Plastics*, chapter 5, Springer, Berlin, Germany, 1987.

[19] E. Fiamegkou, N. Athanasopoulos, and V. Kostopoulos, "Prediction of the effective thermal conductivity of carbon nanotube-reinforced polymer systems," *Polymer Composites*, vol. 35, no. 10, pp. 1997–2009, 2014.

[20] B. Mutnuri, *Thermal conductivity characterization of composite materials [M.S. thesis]*, West Virgina University, College of Engineering and Mineral Resources, 2006.

[21] C.-W. Nan, G. Liu, Y. Lin, and M. Li, "Interface effect on thermal conductivity of carbon nanotube composites," *Applied Physics Letters*, vol. 85, no. 16, pp. 3549–3551, 2004.

[22] J. C. Lagarias, J. A. Reeds, M. H. Wright, and P. E. Wright, "Convergence properties of the Nelder-Mead simplex method in low dimensions," *SIAM Journal on Optimization*, vol. 9, no. 1, pp. 112–147, 1998.